Z-Merge: Multi-Agent Reinforcement Learning for On-Ramp Merging with Zone-Specific V2X Traffic Information

Yassine Ibork¹, Myounggyu Won², Lokesh Das¹

¹School of Computing, Wichita State University
²Department of Computer Science, University of Memphis
yxibork@shockers.wichita.edu, mwon@memphis.edu, lokesh.das@wichita.edu

Abstract

Ramp merging is a critical and challenging task for autonomous vehicles (AVs), particularly in mixed traffic environments with human-driven vehicles (HVs). Existing approaches typically rely on either lane-changing or inter-vehicle gap creation strategies based solely on local or neighboring information, often leading to suboptimal performance in terms of safety and traffic efficiency. In this paper, we present a V2X (vehicle-toeverything communication)-assisted Multiagent Reinforcement Learning (MARL) framework for on-ramp merging that effectively coordinates the complex interplay between lane-changing and inter-vehicle gap adaptation strategies by utilizing zone-specific global information available from a roadside unit (RSU). The merging control problem is formulated as a Multiagent Partially Observable Markov Decision Process (MA-POMDP), where agents leverage both local and global observations through V2X communication. To support both discrete and continuous control decisions, we design a hybrid action space and adopt a parameterized deep Q-learning approach. Extensive simulations, integrating the SUMO traffic simulator and the MOSAIC V2X simulator, demonstrate that our framework significantly improves merging success rate, traffic efficiency, and road safety across diverse traffic scenarios.

Introduction

Ramp merging is a critical maneuver that involves complex interactions between merging vehicles and mainline traffic. According to the U.S. Department of Transportation, approximately 300,000 car accidents occur each year in merging areas, contributing to around 50,000 fatal crashes (el abidine Kherroubi, Aknine, and Bacha 2021). Ramp merging is also a major contributor to traffic congestion, often caused by poor coordination between vehicles and unpredictable driving behavior (Liao et al. 2021). Highway merging accounts for approximately 40–80% of traffic congestion in the U.S., and about 1.7% of traffic fatalities occur during lane change or merging maneuvers (Nakka, Chalaki, and Malikopoulos 2022).

Copyright © 2026, Association for the Advancement of Artificial Intelligence (www.aaai.org). All rights reserved.

With the rapid advancement of autonomous vehicles (AVs), numerous studies have been conducted to control AV motion in merging areas, aiming to enhance traffic efficiency, safety, and driving comfort. Two primary control strategies are inter-vehicle gap adjustment and lane-change maneuvers. Gap control approaches are primarily designed for mainline vehicles to create sufficient space for smooth merging (Das and Won 2021a,b; Yadavalli, Das, and Won 2023; Zhu et al. 2024). Alternatively, lane-change strategies focus on enabling mainline vehicles to change lanes to accommodate merging vehicles, while longitudinal control is typically used only for collision avoidance (Xia et al. 2024; Liu et al. 2024; Cai et al. 2024; Chen and Yang 2024). More recent approaches have focused on integrating both inter-vehicle gap adjustment and lane-change strategies to simultaneously coordinate the lane-change and gap creation for efficient merging. (Wang et al. 2024; Hou et al. 2023; Chen et al. 2023). However, these existing methods rely solely on local sensor data or limited information from neighboring vehicles via standard V2X communication, missing the opportunity to leverage "global" and "zonespecific" information that could significantly enhance traffic efficiency, safety, and driver comfort.

In this paper, we present Z-Merge, a zone-based onramp merging control method using multi-agent reinforcement learning (MARL). The roadway segment is strategically divided into three zones: pre-merging, merging, and ramp. Summarized traffic information from each zone, collected via a roadside unit (RSU), is independently integrated into the MARL framework. This enables agents to make more informed and holistic decisions by combining inter-vehicle gap adjustment and lane-change strategies, thereby facilitating safe, efficient, and smooth on-ramp merging. To the best of our knowledge, this is the first MARL-based merging control method that incorporates both local and zone-specific traffic information. More specifically, we formulate the problem of simultaneously controlling the motion of multiple agents in a merging area—through the complex interplay of lanechanging, acceleration/deceleration, and inter-vehicle gap adaptation—using a Multi-Agent Partially Observable Markov Decision Process (MA-POMDP) framework. The state space is carefully designed, informed by transportation literature, to incorporate critical traffic parameters that capture both local information (i.e., data collected through onboard sensors and vehicle-tovehicle communication) and global (zone-specific) traffic conditions—factors that significantly influence traffic efficiency, safety, and driving comfort. To enable efficient, smooth, and collision-free merging, we design a hybrid action space that integrates lane-changing, acceleration/deceleration, and inter-vehicle gap adjustment controls. A robust multi-agent decision-making algorithm, based on the Parameterized Deep Q-Network (PDQN), is developed to select optimal control policies. We conduct extensive simulations incorporating V2X communication to train and evaluate the reinforcement learning agents. The results demonstrate that the proposed V2X-assisted MARL framework effectively enhances road safety, traffic efficiency, merging success rate, and queue length under complex merging conditions compared with state-of-the-art method. The contributions of our work are summarized as follows.

- We propose the first zone-based on-ramp merging control method using multi-agent reinforcement learning (MARL) incorporating RSU-collected, zone-specific traffic information from pre-merging, merging, and ramp zones.
- We carefully design the state space and hybrid action space to support holistic decision-making: the state space integrates both local and global traffic information, while the hybrid action space includes discrete (lane-change) and continuous (acceleration and gap control) actions.
- We incorporate the Parameterized Deep Q-Network (PDQN) algorithm to achieve end-to-end vehicle control with both discrete and continuous action parameters. We develop a Double Parameterized Deep Q-Network to mitigate overestimation bias and improve learning stability.
- We implement a simulation framework integrating the SUMO traffic simulator (Lopez et al. 2018) with Eclipse MOSAIC (Schrab et al. 2022) to enable realistic V2X communication and conduct extensive simulations under various traffic conditions.

Related Work

A substantial body of research on on-ramp merging control strategies can be broadly categorized into three types: (1) inter-vehicle gap control-based approaches, (2) lane-change-based approaches, and (3) hybrid approaches that combine both. Inter-vehicle gap control strategies primarily focus on adjusting the spacing between vehicles on the mainline to ensure a safe merging gap for ramp vehicles. Das and Won proposed a deep Q-Network-assisted dynamic ACC method that adaptively adjusts inter-vehicle gaps (Das and Won 2021a). They later developed a safety-aware intelligent ACC using dual reinforcement learning agents to dynamically tune the time-to-collision threshold and desired

gaps (Das and Won 2021b). Yadavalli et al. designed a reinforcement learning-based approach for dynamic intra-platoon gap adaptation to support on-ramp merging (Yadavalli, Das, and Won 2023). Zhu et al. introduced a hierarchical gap creation strategy where mainline vehicles decelerate to create space for a platoon formed by ramp vehicles (Zhu et al. 2024). However, these methods are limited to controlling mainline vehicles within the merging zone, often causing upstream congestion—especially in the pre-merging area. Additionally, since they do not account for lateral maneuvers such as lane changes, these approaches are less effective in dynamically allocating road space in dense or highly interactive traffic scenarios.

Another extensively used merging control strategy is the lane-change-based approach, which regulates mandatory lane changes by merging vehicles to enter the mainline and discretionary lane changes by mainline vehicles to create space for merging. Xia et al. proposed a multi-lane on-ramp merging strategy integrating dynamic lane-changing decisions with trajectory optimization (Xia et al. 2024). Liu et al. developed a multi-step cooperative lane-change strategy for connected autonomous vehicle (CAV) platoons approaching the merging zone (Liu et al. 2024). Cai et al. introduced a novel merging control method that also emphasizes mainline lane changing (Cai et al. 2024). Shi et al. formulated a trajectory optimization-based lanechanging policy to enhance merge safety and minimize mainline traffic disruption (Shi et al. 2024). However, these approaches typically depend on local information and lack coordination with upstream traffic, making them less effective in handling dense or rapidly changing traffic conditions. Moreover, without integration with longitudinal gap control, they may cause sudden maneuvers or unsafe cut-ins, reducing overall traffic sta-

A hybrid on-ramp merging strategy that integrates both lane-changing and inter-vehicle gap adjustment has recently attracted increasing attention due to its adaptability, robustness, and efficiency. Wang et al. proposed a cooperative lane-changing framework that combines longitudinal headway adjustment with lateral maneuver execution (Wang et al. 2024). Hou et al. developed a hierarchical model for cooperative merging, where the upper layer identifies suitable merging gaps through anticipatory position-searching, and the lower layer handles lateral control (Hou et al. 2023). Chen et al. incorporated both gap creation and mainline lane changes to facilitate merging operations (Chen et al. 2023). However, despite this promising trend, existing hybrid approaches largely rely on localized information or heuristic coordination, and thus fall short of exploiting the full potential of V2X communication. This limitation motivates the design of Z-Merge, which strategically incorporates zone-specific global traffic information to enable agents to make more holistic and informed merging decisions. By leveraging this broader situational awareness, Z-Merge enhances traffic efficiency, safety, and driving comfort in complex on-ramp merging scenarios.

Design of Z-Merge

In this section, we present the details of Z-Merge. We begin with an operational overview of Z-Merge, followed by the design of our MARL framework. We then describe the implementation of our multi-agent Parameterized Deep Q-Network (PDQN) algorithm.

Overview

This section provides an operational overview of Z-Merge. The system is designed for a roadway segment with an on-ramp, as illustrated in Fig. 1. The segment is divided into three zones: the pre-merging zone, the merging zone, and the on-ramp zone. The traffic environment includes both autonomous vehicles (AVs, i.e., agents) and human-driven vehicles (HVs). A roadside unit (RSU) oversees the entire segment. Each vehicle gathers local information—such as position, speed, heading, and nearby vehicle states—via onboard sensors and vehicle-to-vehicle (V2V) communication, and transmits this information to the RSU through V2X communication. The RSU aggregates the received data to construct zone-specific traffic summaries, which are then made available to AVs to support coordinated and informed decision-making.

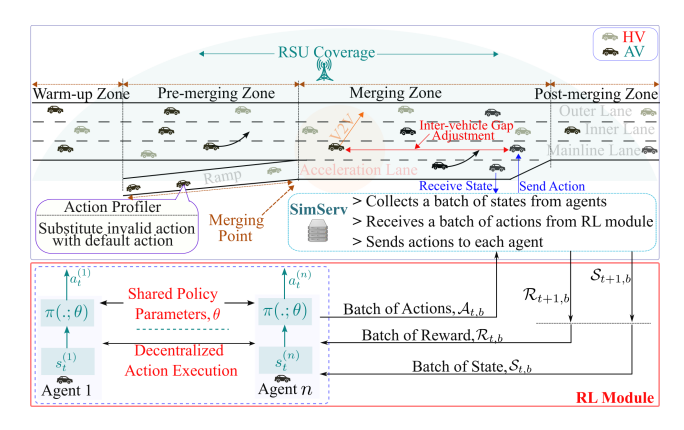


Figure 1: An operational overview of Z-Merge.

Problem Formulation

We model the on-ramp merging problem using the decentralized Partially Observable Markov Decision Process (Dec-POMDP) defined by the tuple, $(S, \{A_i, \mathcal{R}_i, \mathcal{O}_i\}_{i \in \mathcal{N}}, \mathcal{T}, \mathcal{O}, \mathcal{Z})$. Here, \mathcal{N} is the set of agents and S is their common state space. For each agent i, A_i is the action space, $\mathcal{R}_i : S \times A \times S \to \mathbb{R}$ is the reward function, and \mathcal{O}_i is the observation space, with joint counterparts $A = A_1 \times \cdots \times A_n$ and $\mathcal{O} = \mathcal{O}_1 \times \cdots \times \mathcal{O}_n$. The transition kernel $\mathcal{T} : S \times A \times S \to [0, 1]$ gives the probability of moving from $s \in S$ to $s' \in S$ under the joint action $a \in A$, while the observation kernel $\mathcal{Z} : S \times A \times \mathcal{O} \to [0, 1]$ yields the probability of

observing $o \in \mathcal{O}$ given the next state $s' \in \mathcal{S}$ and joint action $a \in \mathcal{A}$. At each step, agent i receives $o_i \in \mathcal{O}_i$ and selects $a_i \in \mathcal{A}_i$, which forms part of the joint action executed in the environment. Each agent seeks a policy $\pi_i : \mathcal{O}_i \to \mathcal{A}_i$ that maximizes its expected discounted long-term reward.

State Space: The state space of agent i at time t, denoted by $S_i^{(t)}$, incorporates both local and global traffic information. The global traffic information includes the average speed and traffic density of the premerging, merging, and ramp zones, as well as the queue lengths of the acceleration lane and mainline within the pre-merging zone. This information is made available to the agent via the RSU. The local information consists of both the ego vehicle's state and the states of surrounding vehicles. The ego vehicle informationincluding speed, acceleration, occupied lane, and time to the merging point—is obtained through onboard sensors. The surrounding vehicle information is represented as $N_i \times F_i$, where N_i is the number of vehicles observed by agent i, and F_i is the feature vector for each observed vehicle, including speed, acceleration, current lane, time to the merging point (MP), and distance to the ego vehicle. This information is obtained via vehicle-to-vehicle (V2V) communication. In particular, we use the Haversine formula to compute the distances from the ego vehicle to surrounding vehicles and to the merging point, which is defined as follows.

$$d = 2r \arcsin\left(\sqrt{\left(\sin^2\left(\frac{\delta\phi}{2}\right) - \cos\phi_1\cos\phi_2\sin^2\left(\frac{\delta\lambda}{2}\right)\right)}\right)$$
(1)

where r is the radius of Earth, $\delta\phi=\phi_1-\phi_2$, where ϕ_1 and ϕ_2 are the latitudes of vehicle 1 and vehicle 2, $\delta\lambda=\lambda_1-\lambda_2$, where λ_1 and λ_2 are the longitudes of vehicle 1 and vehicle 2, respectively. Finally, the complete state space of Z-Merge at time t is the product of all individual agents' state space, i.e., $\mathcal{S}^{(t)}=\mathcal{S}_1^{(t)}\times\mathcal{S}_2^{(t)}\times\mathcal{S}_3^{(t)}\times\ldots\times\mathcal{S}_{n\in\mathcal{N}}^{(t)}$.

Action Space: We design action spaces for both merging and mainline vehicles to enable safe, smooth, and congestion-free on-ramp merging. A hybrid action space is incorporated into our framework, allowing each RL agent to select either a discrete or continuous action. Specifically, an agent's action space is defined as $A_i = \{a_0, a_1, a_2, a_3, a_4\}$, where a_0 denotes a lane change to the left, a_1 denotes a lane change to the right, $a_2 \in [-4.5 \, \text{m/s}^2, 2.6 \, \text{m/s}^2]$ represents acceleration or deceleration, $a_3 \in [5 \, \text{m}, 20 \, \text{m}]$ specifies the desired intervehicle gap, and a_4 indicates maintaining the current state. This hybrid structure enables agents to effectively perform both lateral and longitudinal maneuvers under dynamic traffic conditions.

Reward Function: The reward function \mathcal{R}_i for agent i is composed of six sub-reward components: r_e for traffic efficiency, r_s for driving safety, r_c for driver comfort, r_q

for queue length reduction, r_d for deadlock avoidance, and r_l for the effect of lane-changing behavior, which is defined as follows.

$$\mathcal{R}_{i}^{(t)} = w_{e} r_{e}^{(t)} + w_{s} r_{s}^{(t)} + w_{c} r_{c}^{(t)} + w_{q} r_{q}^{(t)} + w_{d} r_{d}^{(t)} + w_{l} r_{l}^{(t)},$$

where w_e , w_s , w_c , w_q , w_d , and w_l are empirically chosen weighting coefficients. We apply a squashing function to each reward component before weighting, ensuring that the composite reward remains well-scaled and no single component dominates the learning process. Specifically, for each reward component r_k (where k = 1, ..., K), we compute the squashed value as $\tilde{r}_k = \tanh(r_k)$, and the overall reward is then calculated as:

$$\mathcal{R}_i^{(t)} = \sum_{k=1}^K w_k \tilde{r}_k,$$

where, w_k is the weighting coefficient for reward component k.

Efficiency Reward: The efficiency reward $r_e^{(t)}$ consists of local efficiency $e_l^{(t)}$ and global traffic efficiency $e_g^{(t)}$, i.e., $r_e^{(t)} = e_g^{(t)} + e_l^{(t)}$. The global efficiency $e_g^{(t)}$ quantifies effects of actions of agents on overall traffic flow, which is defined in terms of minimum average speed \bar{v}_{e_m} , and maximum average speed, \bar{v}_{e_M} of the road segment, i.e.,

$$e_q^{(t)} = -(|\bar{v}_e - \bar{v}_{e_M}|)/(\bar{v}_{e_M} - \bar{v}_{e_m}).$$

The local efficiency $e_l^{(t)}$ encourages the ego vehicle to maintain a speed close to the maximum speed limit v_M , defined for the road segment, while ensuring collision-free merging, i.e.,

$$e_l^{(t)} = -(|v'(t) - v_M|)/(v_M - v_m),$$

where $v'^{(t)}$ and v'_m are the current speed and the minimum speed of the RL agent, respectively.

Safety Reward: The safety reward function $r_s^{(t)}$ is designed to account for both lateral and longitudinal safety. More specifically, an agent i is penalized at time t if (i) it collides with another vehicle, (ii) its time-to-collision $TTC_i^{(t)}$, defined by (2), with respect to the leading vehicle is within the time-to-collision threshold TTC^* which is set to 1.2s (Ayres et al. 2001) or (iii) its lateral distance $\mathcal{D}_i^{(t)}$, determined by (1), to the target lane leader and follower is less than the lateral safety threshold δ which is set to 12m (Dingus et al. 2006). Otherwise, it receives zero reward.

$$TTC_i^{(t)} = \begin{cases} \frac{(x_{n-1} - x_n - l_{n-1})}{(v_n - v_{n-1})}, & \text{if } v_n > v_{n-1} \\ \infty, & \text{Otherwise,} \end{cases}$$
(2)

where n-1 is the leader vehicle, n is the follower vehicle, x is the longitudinal position, v is the vehicle speed and l is the length of the leader vehicle. Consequently, the safety reward function is defined as follows.

$$r_s^{(t)} = \begin{cases} -1, & \text{if collision} \\ -exp(-TTC_i^{(t)}), & \text{if } TTC_i^{(t)} \leq TTC^* \\ -\delta/\mathcal{D}, & \text{if } \mathcal{D} \leq \delta \\ 0, & \text{otherwise,} \end{cases}$$

Queue Reward: To prevent traffic congestion on the mainline of the pre-merging zone and in the acceleration lane, we penalize an agent if its actions contribute to increased queue lengths in these areas. The queue-based penalty is defined as

$$r_q^{(t)} = -\log_{10}(\mathcal{Q}_p^{(t)} + \mathcal{Q}_a^{(t)}),$$

where $Q_p^{(t)}$ and $Q_a^{(t)}$ represent the queue lengths on the pre-merging zone and in the acceleration lane at time t, respectively.

Driving Comfort: The driving comfort reward function $r_c^{(t)}$, adopted from (Xu et al. 2024), penalizes excessive acceleration or deceleration and is defined as follows.

$$r_c^{(t)} = \begin{cases} -(|\alpha_i^{(t)}| - \alpha_{max})/(|\alpha_i^{(t)}|) & \text{if } |\alpha_i^{(t)}| > \alpha_{max} \\ 0 & \text{otherwise,} \end{cases}$$

where $|\alpha_i^{(t)}|$ denotes the magnitude of the longitudinal acceleration (or deceleration) applied by agent i at time t, and a_{max} is the comfort threshold, set to $2.6 \,\text{m/s}^2$.

Deadlock Penalty: To prevent merging vehicles from remaining stagnant at the end of the acceleration lane, we define the deadlock reward $r_d^{(t)}$ to penalize agents more heavily as they approach the end of the lane, i.e.,

$$r_d^{(t)} = \begin{cases} -exp\Big(-\frac{(x-L)^2}{10L}\Big), & \text{if stay on accel. lane} \\ 0, & \text{otherwise,} \end{cases}$$

where x is the current position of the ego vehicle on the acceleration lane, and L is the length of the acceleration

Lane Change Penalty: Excessive lane changes pose challenges to traffic safety and reduce traffic efficiency. We incorporate a lane change reward function $r_l^{(t)}$ to penalize an agent if it performs unnecessary lane changes, which is defined as follows.

$$r_l^{(t)} = \begin{cases} -1, & \text{if change lanes} \\ 0, & \text{otherwise.} \end{cases}$$

Multi-Agent Parameterized Double DQN

Due to the hybrid nature of our action space, we solve our multi-agent on-ramp merging problem using the Parameterized Deep Q-Network (PDQN) algorithm (Xiong et al. 2018). In particular, we adopt the centralized training with decentralized execution (CTDE) paradigm (Amato 2024), along with a

parameter-sharing mechanism: all agents share a common policy and value network and contribute to a shared replay buffer by recording their experiences at each time step. This approach enables each agent to benefit from a larger and more diverse dataset, which accelerates learning while maintaining decentralized decision-making during execution.

In a hybrid Markov Decision Process (MDP), the action space is defined as a joint space

$$A = \{(k, x_k) \mid k \in \{1, \dots, K\}, x_k \in \mathcal{X}_k\},\$$

where k is a discrete high-level action index and x_k is the corresponding continuous argument. The policy must select both a discrete action and its associated continuous argument. Following (Xiong et al. 2018), we employ an actor–critic architecture: a Q-network $Q_{\phi}(s,k,x_k)$ evaluates state–action–parameter tuples, and a parameter (actor) network $\mu_{\theta}(s) \in \mathbb{R}^{\sum_k d_k}$ outputs a joint vector $x = (x_1, \ldots, x_K)$, where each x_k corresponds to the continuous argument for discrete action k.

At each time step t, the parameter network generates a full vector of continuous parameters $x_t = \mu_{\theta}(s_t)$. The Q-network then computes the Q-values for each discrete action using its corresponding parameter vector component, and selects the action as $k^* = \arg\max_k Q_{\phi}(s_t, k, x_k)$.

To address overestimation bias, we adopt a Double PDQN approach. For each transition (s_t, a_t, r_t, s_{t+1}) , we first select the candidate action using the online critic:

$$k^{\text{online}*} = \arg \max_{k'} Q_{\phi}\left(s_{t+1}, k', \mu_{\theta}(s_{t+1})_{k'}\right),$$

then evaluate it with the target critic:

$$y_t = r_t + \gamma Q_{\phi^-} \left(s_{t+1}, k^{\text{online}*}, \mu_{\theta^-}(s_{t+1})_{k^{\text{online}*}} \right), \quad (3)$$

where ϕ^- and θ^- denote the parameters of the target Q-network and target parameter network, respectively. These target parameters are updated periodically using hard updates every 35,000 gradient steps.

The Q-network is optimized by minimizing the temporal-difference (TD) error:

$$\mathcal{L}_Q = \left(Q_\phi(s_t, k_t, x_{k_t}) - y_t\right)^2.$$

Meanwhile, the parameter network is updated to maximize the expected Q-value by minimizing the negative of the estimated return:

$$\mathcal{L}_{\mu} = -\mathbb{E}_{s \sim \mathcal{D}} \left[Q_{\phi} \left(s, k, \mu_{\theta}(s)_{k} \right) \right].$$

The hyperparameters used in the optimization process are summarized in Table 1.

Simulation Results

Simulation Setup

We employed traffic simulators MOSAIC (Schrab et al. 2022) and SUMO (Lopez et al. 2018) to implement Z-Merge. SUMO is used to simulate the microscopic vehicle dynamics and road traffic environment, whereas

MOSAIC is employed to ensure V2X communication. The MARL framework of Z-Merge was developed using PyTorch. To interface the framework with MOSAICwhich is implemented in Java—we developed a communication module called "SimServ". SimServ acts as a bridge between the simulation environment and the RL module: it aggregates the state information of each RL agent and transmits it to the RL framework. The RL module then processes a batch of states and returns a corresponding batch of actions to SimServ. SimServ forwards each action to the appropriate agent using predefined routing identifiers. Upon receiving an action, each agent invokes an action validation module ("action profiler") to determine whether the action is valid. If the action is deemed invalid, it is replaced with a default fallback action.

We consider a 320 m-long road segment with an onramp, which is divided into a 150 m pre-merging zone and a 100 m merging zone. The on-ramp is 100 m in length. Vehicles use initial 50 m called "warm-up zone" for injecting into the network and adapting the speed limit. Traffic flow rates are set to 3600 and 900 vehicles per hour per lane for the mainline and the ramp, respectively, with vehicle arrivals modeled as a Poisson process. Among all vehicles, 60% are AVs controlled by Z-Merge, while the remaining 40% are HVs governed by MOSAIC's default driving model. Each AV agent makes decisions regarding throttle, braking, and lane changes at intervals of 0.1 s.

We performed hyperparameter tuning to identify the optimal configuration for achieving the best performance. Specifically, we used a grid search method to select the optimal values for the learning rate, discount factor, batch size, replay buffer size, target update frequency, and the number of hidden layers in both the actor and parameter networks. The final hyperparameters used in the simulation are summarized in Table 1.

We validated Z-Merge using five key evaluation metrics: (i) traffic efficiency, (ii) traffic safety, (iii) driving comfort, (iv) success rate, and (v) queue length. We compared our method against three baseline approaches: "lane change" (hereafter, Baseline-1) (Liu et al. 2024), "inter-vehicle gap adjustment" (Baseline-2) (Zhu et al. 2024), and "lane change with inter-vehicle gap adjustment in the merging zone" (Baseline-3) (Wu et al. 2025). Traffic efficiency is measured by the average speed of all vehicles on the highway segment. Traffic safety is quantified by the collision rate, defined as the proportion of AVs that collide with other vehicles during the simulation. Driving comfort reflects the smoothness of driving and is evaluated based on vehicle acceleration and deceleration during the simulation (De Winkel et al. 2023). The success rate is defined as the fraction of vehicles entering from the ramp that successfully merge into the mainline without collisions or coming to a stop. Queue length is defined as the number of consecutive vehicles traveling at speeds below $2 \,\mathrm{m/s}$ (Li et al. 2025).

Table 1: Hyper/parameters for Z-Merge.

Environment Parameters								
V2V & V2X range	(100m, 500m)							
Highway speed limit, v_{max}	32m/s							
Accel. range, (a_{max}, a_{min})	$a \in [2.8, -4.5]m/s^2$							
Simulation time step, Δt	0.1s							
Time gap offset, τ	1s							
RL Parameters								
State space, action space	42, 5							
Hidden layers	[256, 512, 512, 128]							
Activation function	ReLU							
Loss function	Huber Loss							
$(\epsilon_{\mathrm{init}}, \epsilon_{\mathrm{final}}, \epsilon_{\mathrm{decay}})$	(1.0, 0.01, 0.999985)							
Batch size, (b)	64							
Discount factor, (γ)	0.995							
Replay buffer size, \mathcal{B}	100,000							
Learning rate								
(Actor, Actor-Param)	$(1 \times 10^{-4}, 1 \times 10^{-4})$							

Traffic Efficiency

We measured traffic efficiency in terms of the average vehicle speed. Fig. 2 presents the average speed over time for all methods. Initially, the differences among the methods were minimal, as vehicles entered the simulation at the maximum initial speed. However, as traffic density increased, the advantages of coordinated lane-changing and inter-vehicle gap adjustment became more apparent. In particular, Z-Merge consistently achieved 26.05% and 131.34% higher average speed compared to Baseline-1 and Baseline-2, respectively, throughout the simulation. This improvement is attributed to Z-Merge's ability to reduce stopand-go traffic in the pre-merging and merging zones, as illustrated in the space-time diagram for Z-Merge (Fig. 3), which highlights its effective management of the complex interplay between lane changes and intervehicle gap adjustments. In comparison with Baseline-3, Z-Merge achieves slightly better performance by 10%. While the gain is modest, it is still noteworthy given that Z-Merge maintains higher traffic efficiency and also delivers consistently strong results across other evaluation metrics, as discussed in the following sections.

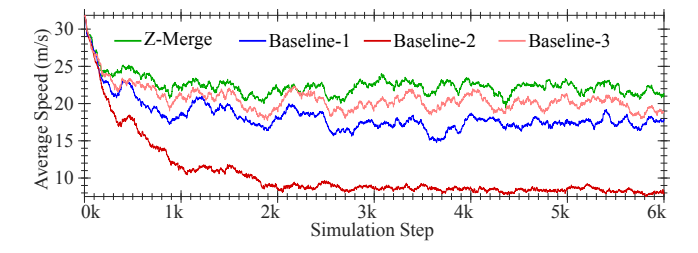


Figure 2: The average speed changes over time.

We also assess the impact of agent penetration rates (PRs) on traffic efficiency, where PRs represent the proportion of AVs relative to HVs in the simulation. Table 2 summarizes the results. Compared to Baseline-1 and

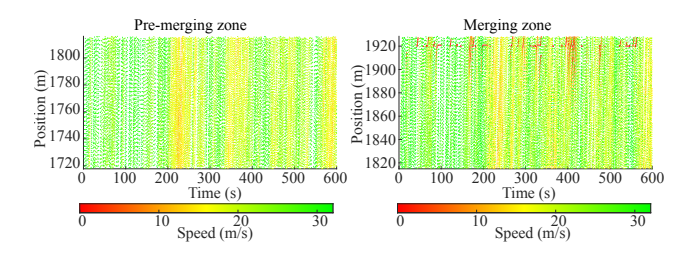


Figure 3: Spatio-temporal representation of the average speed for Z-Merge in pre-merging and merging zones.

Baseline-2, Z-Merge yields significantly higher traffic efficiency—up to a 118.6% improvement—as PRs increase from 5% to 60%. Interestingly, PRs have minimal or even negative effects on traffic efficiency for Baseline-2. This is because, although mainline vehicles create inter-vehicle gaps, some AVs are forced to decelerate, causing congestion in the pre-merging zone. Furthermore, the absence of a lane-change module prevents merging vehicles from utilizing available gaps effectively, leading to congestion in the acceleration lane. We also observe that Baseline-3 performs similar or slightly better than Z-Merge at high PRs, but it struggles to maintain high efficiency at lower PRs. We need to change this line. Notably, this performance gain at high PRs comes at the cost of reduced safety and success rate. This suggests that relying solely on local information can yield higher efficiency but may compromise safety. In contrast, Z-Merge's panoramic control over both the merging and pre-merging zones enables it to achieve high traffic efficiency while also preserving safety and merging success (discussed in the following sections).

Traffic Safety

We evaluated the performance of Z-Merge in terms of traffic safety, measured by the collision rate. The results are summarized in Table 2. Among all approaches, Baseline-2 achieves the best traffic safety, with its collision rate never exceeding 0.11% across all PRs. This is because Baseline-2 only adjusts inter-vehicle gaps and does not perform lane changes, thereby eliminating additional collision risks introduced by lateral maneuvers. In contrast, Baseline-3 exhibits significantly higher collision rates, particularly at low PRs. For example, at a PR of 5%, the collision rate reaches 21.20%. However, the collision rate for Baseline-3 decreases as PR increases, dropping to 4.53% at 60% PR. This trend suggests that a higher presence of AVs mitigates the risk of unsafe interactions, even without global coordination. Z-Merge significantly reduces the collision rate compared to Baseline-3—by up to 57.16%—while achieving safety levels comparable to Baseline-1. Moreover, Z-Merge's collision rate steadily declines as PR increases, reaching 2.66% at 60% PR. This improvement can be attributed to Z-Merge's panoramic coordination across both merging and pre-merging zones. Unlike Baseline-

Table 2: Effect of PRs on the performance of Z-Merge and Baselines.

PR (%)	Z-Merge		Baseline-1		Baseline-2		Baseline-3					
	Efficiency	Safety (%)	Succ. Rate (%)	Efficiency	Safety (%)	Succ. Rate (%)	Efficiency	Safety (%)	Succ. Rate (%)	Efficiency	Safety (%)	Succ. Rate (%)
5	10.65 ± 0.86	6.27 ± 3.79	16.46 ± 6.84	10.24 ± 0.75	11.26 ± 6.88	7.92 ± 5.85	9.56 ± 0.73	0.00 ± 0.00	16.42 ± 4.10	9.82 ± 1.02	6.32 ± 3.82	17.50 ± 5.85
10	12.31 ± 1.42	5.31 ± 3.20	25.31 ± 7.63	11.35 ± 0.87	9.06 ± 3.74	28.19 ± 5.75	9.43 ± 0.73	$\boldsymbol{0.07 \pm 0.31}$	20.92 ± 4.14	9.06 ± 2.01	4.95 ± 2.63	20.82 ± 5.20
20	16.38 ± 1.68	4.99 ± 2.01	51.15 ± 11.20	13.24 ± 1.29	6.88 ± 1.98	43.42 ± 5.93	9.41 ± 0.57	0.10 ± 0.32	28.16 ± 4.48	12.15 ± 3.71	5.01 ± 1.78	38.84 ± 11.10
40	21.58 ± 0.91	4.26 ± 1.29	85.23 ± 4.99	17.12 ± 1.82	3.52 ± 1.46	76.51 ± 7.90	9.34 ± 0.72	0.02 ± 0.08	45.47 ± 5.36	19.61 ± 2.99	6.13 ± 1.69	73.61 ± 6.65
60	23.28 ± 0.78	2.66 ± 0.88	93.25 ± 2.85	18.10 ± 1.33	2.14 ± 0.87	89.51 ± 4.75	9.12 ± 0.91	0.07 ± 0.13	59.36 ± 5.03	22.38 ± 1.10	6.21 ± 1.35	82.61 ± 4.68

3, which allows full local control of lane changes and gap adjustments but lacks information from surrounding zones, Z-Merge leverages cross-zone information to proactively manage interactions and reduce conflicts.

Driving Comfort

To evaluate driving comfort, we analyze the acceleration profiles of vehicles injected into the simulation at three representative time points: 200 s, 290 s, and 360 s. For each time point, we track one mainline vehicle and one ramp vehicle that experience the highest variation in acceleration or deceleration. The resulting profiles are shown in Fig. 4. It is evident that AVs controlled by Z-Merge exhibit smoother and more continuous acceleration patterns. In particular, mainline vehicles maintain a gentle acceleration profile, while ramp vehicles experience minimal fluctuations. In contrast, AVs using Baseline-1 and Baseline-2 show sharp acceleration changes, especially within the merging zone (i.e., positions between 18301950 m). Baseline-3 also struggles to maintain smooth acceleration, particularly for mainline vehicles. Notably, Z-Merge maintains acceleration within the comfortable driving range. According to (De Winkel et al. 2023), a comfortable acceleration threshold is defined as 1.47 m/s², and accelerations up to $2.12\,\mathrm{m/s}^2$ are considered acceptable. Z-Merge stays well within these limits across all scenarios.

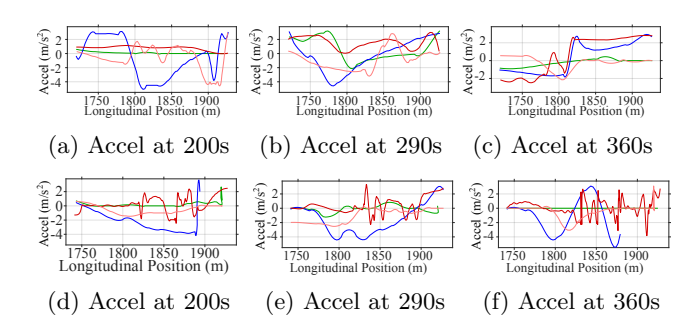
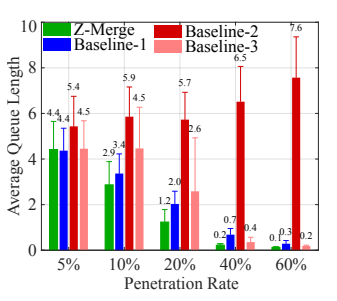


Figure 4: Acceleration trajectories for vehicles at three different time instances. The top row presents the acceleration profile of a merging vehicle, whereas the bottom row presents that of a mainline vehicle. — Z-Merge, — Baseline-1, — Baseline-2, — Baseline-3.

Queue Length

We measured the average queue length with respect to varying PRs. Fig. 5 shows the results. We observe that queue length decreases for Baseline-1, Baseline-3, and Z-Merge as PRs increase, primarily because the growing presence of AVs enables smoother merging and reduced stop-and-go behavior. Interestingly, however, the queue length for Baseline-2 increases with higher PRs. This is because Baseline-2 relies heavily on creating larger inter-vehicle gaps to facilitate merging, which causes upstream vehicles to decelerate and contributes to longer queues. Overall, Z-Merge achieves the shortest queue lengths across all PR levels, outperforming Baseline-1, Baseline-2, and Baseline-3 by up to 65.51%, 98.68%, and 50%, respectively. These results highlight the effectiveness of combining zone-specific global information with synchronized control of both lane-changing and inter-vehicle gap adjustment.



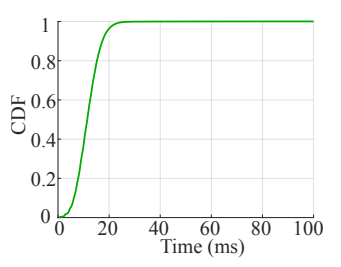


Figure 5: Avg. queue length.

Figure 6: Computational overhead.

Success Rate

The success rate indicates the proportion of vehicles that successfully enter the mainline without stopping at the end of the acceleration lane or colliding with other vehicles. As shown in Table 2, the success rate of Z-Merge increases significantly with higher PRs of AVs on both the ramp and the mainline. Specifically, Z-Merge improves the success rate from 16.4% at a PR of 5% to 93.25% at 60%, representing a relative gain of 466.52%. Although Baseline-1, Baseline-2, and Baseline-3 also show improvement with increasing PRs, their success rates remain substantially lower than that of Z-Merge. On average, they underperform Z-Merge

by 4.17%, 57.09%, and 12.87%, respectively. This performance gap can be attributed to their limited capabilities: Baseline-1 and Baseline-2 rely solely on either lane-changing or inter-vehicle gap adjustment, while Baseline-3 lacks access to global, zone-specific information. As a result, these baselines struggle to coordinate effectively in the dynamic and complex context of onramp merging.

Computational Overhead

Agents must make decisions rapidly on high-speed roadways. In particular, continuous control over lane changes and inter-vehicle gap adjustments in complex and dynamically evolving scenarios—such as onramp merging—requires minimal computational delay. In this section, we measured the inference time of the RL decision-making process. Specifically, we evaluated the per-step decision interval over 6,000 iterations on a Mac Mini equipped with an M4-Pro chip and 48 GB of RAM. Each cycle includes (i) processing the current batch of states, (ii) computing the corresponding actions, (iii) sending actions to the environment, and (iv) receiving the next states. Fig. 6 presents the cumulative distribution function (CDF) of the per-step inference time. The results indicate that in 90% of cases, the inference time remains below 16 ms, with an average delay of 11.70 ms. Overall, the observed computational latency is sufficiently low to support real-time decision-making in high-speed traffic environments.

Conclusion

We presented Z-Merge, a MARL framework designed to enhance the efficiency of on-ramp merging through synchronized lane-change and inter-vehicle gap adjustment strategies. By leveraging zone-specific global information and centralized training with decentralized execution, Z-Merge demonstrated superior performance across multiple metrics—including traffic efficiency, safety, driving comfort, success rate, and queue length—when compared to existing baselines. Extensive simulation results under varying penetration rates confirmed the effectiveness of Z-Merge. Furthermore, inference time analysis showed that Z-Merge operates within real-time constraints, making it suitable for high-speed driving environments.

References

- Amato, C. 2024. An introduction to centralized training for decentralized execution in cooperative multi-agent reinforcement learning. arXiv preprint arXiv:2409.03052.
- Ayres, T.; Li, L.; Schleuning, D.; and Young, D. 2001. Preferred time-headway of highway drivers. In ITSC 2001. 2001 IEEE Intelligent Transportation Systems. Proceedings (Cat. No. 01TH8585), 826–829. IEEE.
- Cai, B.; Cao, Y.; Chai, L.; Shangguan, W.; Cao, Y.; Gao, J.; and Chen, J. 2024. A Graph Reinforcement

- Leaning-Based Approach for Merging of Mixed Traffic Vehicles on On-Ramp. In 2024 IEEE 27th International Conference on Intelligent Transportation Systems (ITSC), 1885–1890. IEEE.
- Chen, D.; Hajidavalloo, M. R.; Li, Z.; Chen, K.; Wang, Y.; Jiang, L.; and Wang, Y. 2023. Deep multi-agent reinforcement learning for highway on-ramp merging in mixed traffic. IEEE Transactions on Intelligent Transportation Systems, 24(11): 11623–11638.
- Chen, R.; and Yang, Z. 2024. Cooperative Ramp Merging Strategy at Multi-Lane Area for Automated Vehicles. IEEE Transactions on Vehicular Technology.
- Das, L.; and Won, M. 2021a. D-ACC: Dynamic Adaptive Cruise Control for Highways with Ramps Based on Deep Q-Learning. In 2021 IEEE International Conference on Robotics and Automation (ICRA), 1572–1578. IEEE.
- Das, L. C.; and Won, M. 2021b. Saint-acc: Safety-aware intelligent adaptive cruise control for autonomous vehicles using deep reinforcement learning. In International Conference on Machine Learning, 2445–2455. PMLR.
- De Winkel, K. N.; Irmak, T.; Happee, R.; and Shyrokau, B. 2023. Standards for passenger comfort in automated vehicles: Acceleration and jerk. Applied Ergonomics, 106: 103881.
- Dingus, T. A.; Klauer, S. G.; Neale, V. L.; Petersen, A.; Lee, S. E.; Sudweeks, J.; Perez, M. A.; Hankey, J.; Ramsey, D.; Gupta, S.; et al. 2006. The 100-car naturalistic driving study, Phase II-results of the 100-car field experiment. Technical report, United States. Department of Transportation. National Highway Traffic Safety
- el abidine Kherroubi, Z.; Aknine, S.; and Bacha, R. 2021. Novel decision-making strategy for connected and autonomous vehicles in highway on-ramp merging. IEEE Transactions on Intelligent Transportation Systems, 23(8): 12490–12502.
- Hou, K.; Zheng, F.; Liu, X.; and Guo, G. 2023. Cooperative on-ramp merging control model for mixed traffic on multi-lane freeways. IEEE Transactions on Intelligent Transportation Systems, 24(10): 10774–10790.
- Li, X.; Wang, X.; Smirnov, I.; Sanner, S.; and Abdulhai, B. 2025. Multi-hop Upstream Anticipatory Traffic Signal Control with Deep Reinforcement Learning. IEEE Open Journal of Intelligent Transportation Systems.
- Liao, X.; Zhao, X.; Wang, Z.; Han, K.; Tiwari, P.; Barth, M. J.; and Wu, G. 2021. Game theory-based ramp merging for mixed traffic with unity-sumo cosimulation. IEEE Transactions on Systems, Man, and Cybernetics: Systems, 52(9): 5746–5757.
- Liu, L.; Li, X.; Li, Y.; Li, J.; and Liu, Z. 2024. Reinforcement Learning-Based Multi-Lane Cooperative Control for On-Ramp Merging in Mixed-Autonomy Traffic. IEEE Internet of Things Journal.
- Lopez, P. A.; Behrisch, M.; Bieker-Walz, L.; Erdmann, J.; Flötteröd, Y.-P.; Hilbrich, R.; Lücken, L.; Rummel,

- J.; Wagner, P.; and Wießner, E. 2018. Microscopic traffic simulation using sumo. In 2018 21st international conference on intelligent transportation systems (ITSC), 2575–2582. Ieee.
- Nakka, S. K. S.; Chalaki, B.; and Malikopoulos, A. A. 2022. A multi-agent deep reinforcement learning coordination framework for connected and automated vehicles at merging roadways. In 2022 American control conference (ACC), 3297–3302. IEEE.
- Schrab, K.; Neubauer, M.; Protzmann, R.; Radusch, I.; Manganiaris, S.; Lytrivis, P.; and Amditis, A. J. 2022. Modeling an its management solution for mixed highway traffic with eclipse mosaic. IEEE Transactions on Intelligent Transportation Systems, 24(6): 6575–6585.
- Shi, J.; Luo, Y.; Li, P.; Wang, J.; and Li, K. 2024. Collaborative multi-lane on-ramp merging strategy for connected and automated vehicles using dynamic conflict graph. Journal of Intelligent and Connected Vehicles.
- Wang, Z.; Xiang, J.; Wang, J.; Gao, Z.; Chen, T.; Li, H.; and Mao, R. 2024. Cooperative Lane-Changing Control for CAVs at Freeway On-Ramps considering Vehicle Dynamics. Journal of Advanced Transportation, 2024(1): 1221717.
- Wu, Q.; Ji, M.; Fan, P.; Wang, K.; Cheng, N.; Chen, W.; and Letaief, K. B. 2025. PPO-Based Vehicle Control for Ramp Merging Scheme Assisted by Enhanced C-V2X. arXiv preprint arXiv:2501.12656.
- Xia, S.; Min, H.; Wu, X.; Fang, Y.; Wang, W.; Xu, Z.; and Zhao, X. 2024. On-ramp Merging Strategy Integrating Dynamic Lane-changing Decision and Quasiuniform B-spline Trajectory Optimization. IEEE Transactions on Vehicular Technology.
- Xiong, J.; Wang, Q.; Yang, Z.; Sun, P.; Han, L.; Zheng, Y.; Fu, H.; Zhang, T.; Liu, J.; and Liu, H. 2018. Parametrized deep q-networks learning: Reinforcement learning with discrete-continuous hybrid action space. arXiv preprint arXiv:1810.06394.
- Xu, D.; Zhang, B.; Qiu, Q.; Li, H.; Guo, H.; and Wang, B. 2024. Graph-based multi agent reinforcement learning for on-ramp merging in mixed traffic. Applied Intelligence, 54(8): 6400–6414.
- Yadavalli, S. R.; Das, L. C.; and Won, M. 2023. Rlpg: Reinforcement learning approach for dynamic intraplatoon gap adaptation for highway on-ramp merging. In 2023 IEEE/RSJ International Conference on Intelligent Robots and Systems (IROS), 5514–5521. IEEE.
- Zhu, J.; Wang, L.; Tasic, I.; and Qu, X. 2024. Improving freeway merging efficiency via flow-level coordination of connected and autonomous vehicles. IEEE Transactions on Intelligent Transportation Systems, 25(7): 6703–6715.